Optics Letters

Experimental demonstration of the conversion of local and correlated Gaussian quantum coherence

Haijun Kang,[1,2] Yang Liu,[1,2] Dongmei Han,[1,2] Na Wang,[1,2] and Xiaolong Su[1,2,*]

[1]State Key Laboratory of Quantum Optics and Quantum Optics Devices, Institute of Opto-Electronics, Shanxi University, Taiyuan 030006, China
[2]Collaborative Innovation Center of Extreme Optics, Shanxi University, Taiyuan, Shanxi 030006, China
*Corresponding author: suxl@sxu.edu.cn

Received 22 April 2021; revised 30 June 2021; accepted 4 July 2021; posted 6 July 2021 (Doc. ID 428597); published 2 August 2021

Quantum coherence plays an important role in quantum information processing. In this Letter, we experimentally demonstrate the conversion of local and correlated Gaussian quantum coherence in the process of converting two squeezed states into an entangled state. We also investigate the relationship among total, local, and correlated coherence and show that the total coherence of a two-mode Gaussian state is the sum of local quantum coherence of each mode and the correlated quantum coherence between two modes. Our results highlight the connection of different quantum coherence in a two-mode Gaussian system and provide references for potential application.

https://doi.org/10.1364/OL.428597

The concept of coherence is the basis for the phenomenon of interference and diffraction in classical wave mechanics. When the superposition principle is applied to quantum mechanics, the concept of quantum coherence is developed [1]. Quantum coherence, which characterizes the quantumness and underpins quantum correlations in quantum systems, plays a key role in many novel quantum phenomena and has been identified as a quantum resource for quantum information processing [2,3]. The relationship between quantum coherence and the complementarity relation [4], uncertainty relation [5], quantum entanglement, or other types of quantum correlation [6–8] has been well studied. Recently, experimental demonstrations obtaining maximal coherence via an assisted distillation process [9], relation between coherence and path information [10], cyclic interconversion between coherence and quantum correlations [11], and quantification of the coherence of a tunable quantum detector [12] have been realized.

The quantum coherence of a quantum state is defined as the minimum distance between the quantum state and an incoherent state in Hilbert space [1], which is different from the visibility of interference in classical optics. There are several methods to quantify quantum coherence that include relative entropy, l_1-norm [1], fisher information [13], and robustness of coherence [14]. The quantization of quantum coherence has also been extended to infinite dimension [15–17].

Quantum coherence can describe the quantum properties of single-mode, two-mode and multi-mode, which is different from quantum correlation that requires at least two modes. In a multi-mode system, local coherence represents the quantum coherence of each mode, and correlated coherence refers to the total correlation (including quantum and classical correlation) among all modes [18–20]. The quantum correlated coherence in a cavity optomechanical system [19], multipartite photonic system [21], and quantum dots system [22] have been investigated. However, the distribution and conversion of local and correlation coherence in a two-mode system are still unclear and have not been experimentally demonstrated.

Gaussian states, such as a squeezed state and Einstein–Podolsky–Rosen (EPR) entangled state, play essential roles in quantum information with continuous variables [23,24]. Gaussian quantum information has made significant progress in quantum teleportation [25,26], quantum dense coding [27,28], quantum entanglement swapping [29–31], quantum key distribution [32–34], quantum computation [35,36], and quantum networks [37]. It has been shown that quantum coherence with continuous variables can be quantified by relative entropy [15,16] Bures and Hellinger distances [17]. The scheme of generating quantum coherence in continuous variable systems via Gaussian measurements has also been proposed [38]. It is important for the investigation of the monogamy and polygamy relation of quantum coherence.

In this Letter, we experimentally demonstrate the conversion of local and correlated Gaussian quantum coherence by coupling two squeezed states on a variable beam splitter. The local and correlated quantum coherence of the two-mode Gaussian state are quantified by relative entropy. We observe that the local quantum coherence of a squeezed state still exists when squeezing disappears with the change of transmissivity of the beam splitter. We demonstrate that the total coherence of a two-mode Gaussian state is the sum of the local quantum coherence of each mode and the correlated quantum coherence between the two modes. Our results highlight the conversion of local and correlated coherence along with the transformation of quantum states and the relation among total, local, and correlated coherence in a two-mode Gaussian state.

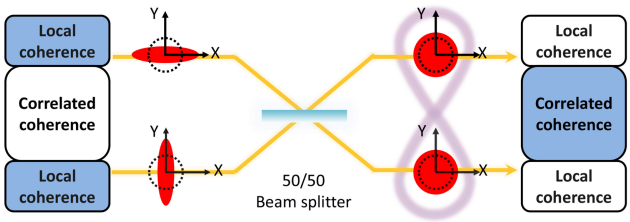

Fig. 1. Schematic of the conversion between local and correlated Gaussian quantum coherence when two squeezed states are converted into an entangled state by a beam splitter. Blue and white boxes represent with and without quantum coherence, respectively. The dotted circle, red ellipse, and circle represent the noise of vacuum, squeezed, and thermal states in phase space, respectively.

As shown in Fig. 1, two squeezed states are coupled on a beam splitter, and an entangled state is obtained when transmittance of the beam splitter is 50%. Only local coherence exists for two independent squeezed states before the beam splitter. When the entangled state is generated, the local coherence converts into correlated coherence totally after the beam splitter.

Here, we use relative entropy to measure the distance in Hilbert space. The relative entropy of quantum coherence of a quantum state $\hat{\rho}$ can be calculated by $\mathcal{C}(\hat{\rho}) = S(\hat{\rho}_{\text{diag}}) - S(\hat{\rho})$, where S is van Neumann entropy, and $\hat{\rho}_{\text{diag}}$ is an incoherent state removing all off-diagonal elements of $\hat{\rho}$ [1]. Total quantum coherence in quantum state $\hat{\rho}_{AB}$ can be represented as [18,19]

$$\mathcal{C}_t(\hat{\rho}_{AB}) = \mathcal{C}_l(\hat{\rho}_{AB}) + \mathcal{C}_c(\hat{\rho}_{AB}), \tag{1}$$

where $\mathcal{C}_t(\hat{\rho}_{AB})$ is total coherence, $\mathcal{C}_l(\hat{\rho}_{AB}) = \mathcal{C}(\hat{\rho}_A) + \mathcal{C}(\hat{\rho}_B)$ is local coherence, and $\mathcal{C}_c(\hat{\rho}_{AB})$ is correlated coherence. The quantum correlated coherence of $\hat{\rho}_{AB}$ is equal to zero, if and only if $\hat{\rho}_{AB} = \hat{\rho}_A \otimes \hat{\rho}_B$ [39].

A Gaussian state can be completely represented by its displacement $\bar{\mathbf{x}}$ and covariance matrix $\mathbf{V}$ in phase space, which correspond to the first and second statistical moments of the quadrature operators, respectively [23,24]. The displacement $\bar{\mathbf{x}} = \langle \hat{\mathbf{x}} \rangle$, where $\hat{\boldsymbol{x}} = (\hat{X}_1, \hat{P}_1, \ldots, \hat{X}_N, \hat{P}_N)^T$, $\hat{X}_k = (\hat{a}_k + \hat{a}_k^\dagger)$ and $\hat{P}_k = i(\hat{a}_k^\dagger - \hat{a}_k)$ are amplitude and phase quadrature of an optical mode, respectively. The elements of $\mathbf{V}$ are defined as $\mathbf{V}_{ij} = \frac{1}{2}\langle \hat{x}_i \hat{x}_j + \hat{x}_j \hat{x}_i \rangle - \langle \hat{x}_i \rangle \langle \hat{x}_j \rangle$. Since the displacements $\bar{\mathbf{x}}$ of the Gaussian states we used in our experiment are zero, the Gaussian state can be completely represented by its covariance matrix $\mathbf{V}$. A typical incoherent state of Gaussian states is the thermal state [16], so it can be used to quantify quantum coherence of Gaussian states. Thus, Gaussian quantum coherence of an N-mode Gaussian state can be represented as [16]

$$\mathcal{C}[\mathbf{V}] = S[\mathbf{V}_{\text{th}}] - S[\mathbf{V}], \tag{2}$$

where $S(\mathbf{V}) = -\sum_{i=1}^{N}\left[\left(\frac{\nu_i-1}{2}\right)\log_2\left(\frac{\nu_i-1}{2}\right) - \left(\frac{\nu_i+1}{2}\right)\log_2\left(\frac{\nu_i+1}{2}\right)\right]$ and $S(\mathbf{V}_{\text{th}}) = -\sum_{i=1}^{N}\left[\left(\frac{\mu_i-1}{2}\right)\log_2\left(\frac{\mu_i-1}{2}\right) - \left(\frac{\mu_i+1}{2}\right)\log_2\left(\frac{\mu_i+1}{2}\right)\right]$ are the von Neumann entropy of a Gaussian state with covariance matrix $\mathbf{V}$ and a thermal state with covariance matrix $\mathbf{V}_{\text{th}}$, respectively. ν_i and μ_i are symplectic eigenvalues of $\mathbf{V}$ and $\mathbf{V}_{\text{th}}$, respectively. Here the elements of the covariance matrix $\mathbf{V}_{\text{th}}$ are given by $\mathbf{V}$ with $V_{\text{th}\,2i-1,2i-1} = V_{\text{th}\,2i,2i} = \frac{1}{2}(V_{2i-1,2i-1} + V_{2i,2i})$.

When an amplitude squeezed state (mode 1) and a phase squeezed state (mode 2) are coupled on a variable beam splitter with zero relative phase difference, the covariance matrix of output modes A and B of the beam splitter is given by

$$\mathbf{V}_{AB} = \begin{pmatrix} \mathbf{V}_A & \mathbf{C} \\ \mathbf{C}^T & \mathbf{V}_B \end{pmatrix}, \tag{3}$$

where $\mathbf{V}_A = \text{diag}\{\langle\delta^2\hat{X}_A\rangle, \langle\delta^2\hat{P}_A\rangle\}$ and $\mathbf{V}_B = \text{diag}\{\langle\delta^2\hat{X}_B\rangle, \langle\delta^2\hat{P}_B\rangle\}$ are the covariance matrices of modes A and B, respectively, and $\mathbf{C} = \text{diag}\{\langle\hat{X}_A\hat{X}_B\rangle, \langle\hat{P}_A\hat{P}_B\rangle\}$ represents the correlation between modes A and B. The variances of amplitude and phase quadratures of modes A and B are given by

$$\langle\delta^2\hat{X}_A\rangle = (1-\eta)\langle\delta^2\hat{X}_1\rangle + \eta\langle\delta^2\hat{X}_2\rangle, \tag{4}$$

$$\langle\delta^2\hat{P}_A\rangle = (1-\eta)\langle\delta^2\hat{P}_1\rangle + \eta\langle\delta^2\hat{P}_2\rangle, \tag{5}$$

$$\langle\delta^2\hat{X}_B\rangle = \eta\langle\delta^2\hat{X}_1\rangle + (1-\eta)\langle\delta^2\hat{X}_2\rangle, \tag{6}$$

$$\langle\delta^2\hat{P}_B\rangle = \eta\langle\delta^2\hat{P}_1\rangle + (1-\eta)\langle\delta^2\hat{P}_2\rangle, \tag{7}$$

where η is transmissivity of the variable beam splitter. $\langle\delta^2\hat{X}_1\rangle$, $\langle\delta^2\hat{P}_1\rangle$, $\langle\delta^2\hat{X}_2\rangle$, and $\langle\delta^2\hat{P}_2\rangle$ are the variances of amplitude and phase quadratures of modes 1 and 2, respectively.

The correlation of the amplitude and phase quadratures of modes A and B are

$$\langle\hat{X}_A\hat{X}_B\rangle = \sqrt{\eta(1-\eta)}(\langle\delta^2\hat{X}_2\rangle - \langle\delta^2\hat{X}_1\rangle), \tag{8}$$

$$\langle\hat{P}_A\hat{P}_B\rangle = \sqrt{\eta(1-\eta)}(\langle\delta^2\hat{P}_2\rangle - \langle\delta^2\hat{P}_1\rangle). \tag{9}$$

Total, local, and correlated quantum coherence of a two-mode Gaussian state are given by

$$\mathcal{C}_t[\mathbf{V}_{AB}] = S(\mathbf{V}_{\text{th}\,AB}) - S(\mathbf{V}_{AB}), \tag{10}$$

$$\mathcal{C}_l[\mathbf{V}_{AB}] = \mathcal{C}[\mathbf{V}_A] + \mathcal{C}[\mathbf{V}_B], \tag{11}$$

$$\mathcal{C}_c[\mathbf{V}_{AB}] = S(\mathbf{V}_A) + S(\mathbf{V}_B) - S(\mathbf{V}_{AB}), \tag{12}$$

where

$$\mathcal{C}[\mathbf{V}_A] = S(\mathbf{V}_{\text{th}\,A}) - S(\mathbf{V}_A), \tag{13}$$

$$\mathcal{C}[\mathbf{V}_B] = S(\mathbf{V}_{\text{th}\,B}) - S(\mathbf{V}_B) \tag{14}$$

are quantum coherence of modes A and B, respectively. The symplectic eigenvalue of $\mathbf{V}_{A(B)}$ is determined by $\sqrt{\text{Det}\mathbf{V}_{A(B)}}$. The symplectic eigenvalues of $\mathbf{V}_{AB}$ can be determined by $\sqrt{\frac{\Delta \pm \sqrt{\Delta^2 - 4\text{Det}\mathbf{V}_{AB}}}{2}}$, where $\Delta = \text{Det}\mathbf{V}_A + \text{Det}\mathbf{V}_B + 2\text{Det}\mathbf{C}$.

As shown in Fig. 2, an amplitude squeezed state and a phase squeezed state, generated from two nondegenerate optical parametric amplifiers (NOPAs), are used to investigate the conversion of Gaussian quantum coherence in our experiment. The NOPA cavity is in a semi-monolithic structure composed of a potassium titanyl phosphate (KTP) crystal whose front surface is used as an input mirror and a concave mirror with curvature radius of 50 mm. NOPA1 and NOPA2 are operated

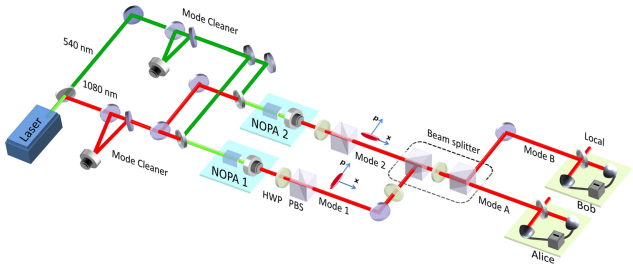

Fig. 2. Experimental setup. The 1080 nm and 540 nm laser beams and are injected into two nondegenerate optical parametric amplifiers (NOPAs) as signal and pump light, respectively. Two squeezed states are coupled on a variable beam splitter. Output modes of the beam splitter are measured by two homodyne detectors simultaneously.

in the case of deamplification and amplification, where the relative phase between the signal and the pump light are locked to $(2n+1)\pi$ and $2n\pi$, respectively. When both half-wave plates (HWPs) behind NOPA1 and NOPA2 are set to 22.5°, the transmitted modes of the two polarization beam splitters (PBSs) are an amplitude squeezed state (mode 1) and a phase squeezed state (mode 2), respectively. Then, we couple modes 1 and 2 to the variable beam splitter, where the variable beam splitter is simulated by the combination of a HWP and two PBSs, and the transmissivity is changed by rotating the HWP.

To reconstruct the covariance matrices of $\mathbf{V}_A$ and $\mathbf{V}_B$, we measure the quantum variance of amplitude quadratures $\langle\delta^2\hat{X}_A\rangle$ and $\langle\delta^2\hat{X}_B\rangle$ and phase quadratures $\langle\delta^2\hat{P}_A\rangle$ and $\langle\delta^2\hat{P}_B\rangle$ in the time domain. Since there is no correlation between amplitude quadrature $\hat{X}_{A(B)}$ and phase quadrature $\hat{P}_{A(B)}$, the non-diagonal elements of $\mathbf{V}_A$ and $\mathbf{V}_B$ are zero. So, we only experimentally measure the diagonal elements in the covariance matrix of mode $A(B)$, which is called partial reconstruction of the covariance matrix [40]. It should be noted that this approximate treatment does not affect the experimental results. The quantum variances of amplitude quadrature $\langle\delta^2\hat{X}_{A(B)}\rangle$ and phase quadrature $\langle\delta^2\hat{P}_{A(B)}\rangle$ are obtained from the measured $\hat{X}_{A(B)}$ and $\hat{P}_{A(B)}$ in the time domain by locking the relative phase of mode $A(B)$ and local oscillator of the homodyne detector to 0 and $\pi/2$, respectively. To reconstruct the covariance matrices of $\mathbf{V}_{AB}$, we also measure cross correlations $\langle\hat{X}_A\hat{X}_B\rangle$ and $\langle\hat{P}_A\hat{P}_B\rangle$ in the time domain. Since there is no correlation between $\hat{X}_{A(B)}$ and $\hat{P}_{B(A)}$, the non-diagonal elements of $\mathbf{C}$ are zero too. The cross correlations are obtained by $\langle\hat{X}_A\hat{X}_B\rangle = [\langle\delta^2\hat{X}_A\rangle + \langle\delta^2\hat{X}_B\rangle - \langle\delta^2(\hat{X}_A - \hat{X}_B)\rangle]/2$ and $\langle\hat{P}_A\hat{P}_B\rangle = [\langle\delta^2\hat{P}_A\rangle + \langle\delta^2\hat{P}_B\rangle - \langle\delta^2(\hat{P}_A - \hat{P}_B)\rangle]/2$, where $\langle\delta^2(\hat{X}_A - \hat{X}_B)\rangle$ and $\langle\delta^2(\hat{P}_A - \hat{P}_B)\rangle$ are obtained from the simultaneously measured amplitude and phase quadrature of modes A and B [40].

In the measurement of output states in the time domain, the electrical signal of each homodyne detector is mixed with a 3 MHz reference signal (SRS, DS345), then passed through a low-pass filter and a low-noise preamplifier (SRS, SR560), and finally recorded in a digital storage oscilloscope (TELEDYNE LECROY, WaveRunner 640Zi). The sampling rate is 500 KS/s, and there are 5×10^5 data for each sampling.

Quantum noises of modes A and B, obtained from the measured quantum variance of amplitude and phase quadratures $\langle\delta^2\hat{x}_i\rangle$ ($\hat{x}_i$ represents $\hat{X}_A$, $\hat{P}_A$, $\hat{X}_B$, and $\hat{P}_B$) according to

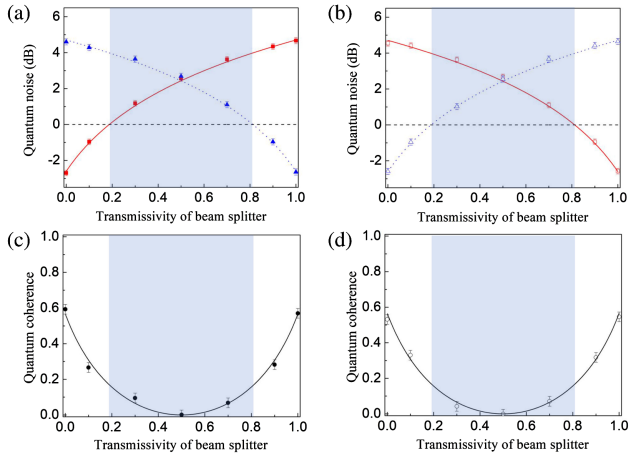

Fig. 3. (a), (b) Dependence of quantum noise of modes A and B on transmissivity of beam splitter, respectively. The solid and dotted curves are quantum noise level of phase and amplitude quadrature, respectively. The black dashed line is shot noise limit (SNL), which corresponds to vacuum noise. (c), (d) Dependence of quantum coherence of modes A and B on transmissivity of beam splitter, respectively. Dots, squares, and triangles correspond to experimental results.

$10\log_{10}\langle\delta^2\hat{x}_i\rangle$ dB, are shown in Figs. 3(a) and 3(b), respectively. We show that quantum noises of phase quadrature of mode A [solid red curve in Fig. 3(a)] and amplitude quadrature of mode B [dotted blue curve in Fig. 3(b)] both increase with the increase in transmissivity η. Conversely, quantum noises of amplitude quadrature of mode A [dotted blue curve in Fig. 3(a)] and phase quadrature of mode B [solid red curve in Fig. 3(b)] decrease with the increase in η. In our experiment, when $\eta = 0$, modes A and B are exactly modes 1 and 2, respectively, since modes 1 and 2 are reflected totally by the beam splitter. Similarly, when $\eta = 1$, modes A and B are exactly modes 2 and 1, respectively, since modes 1 and 2 are transmitted totally by the beam splitter. So, squeezing is observed at $\eta = 0$ and $\eta = 1$. The squeezing and anti-squeezing of modes 1 and 2 are -2.6 ± 0.08 dB ($\langle\delta^2\hat{P}_1\rangle = \langle\delta^2\hat{X}_2\rangle \approx 0.55$) and 4.7 ± 0.08 dB ($\langle\delta^2\hat{X}_1\rangle = \langle\delta^2\hat{P}_2\rangle \approx 2.95$), respectively.

Quantum coherences of modes A and B, obtained according to Eqs. (13) and (14) based on the measured covariance matrices $\mathbf{V}_A$ and $\mathbf{V}_B$, are shown in Figs. 3(c) and 3(d), respectively. Squeezing of modes A and B exists in the regions of $0 \le \eta < 0.188$ and $0.812 < \eta \le 1$. It is interesting that squeezing disappears in the region of $0.188 \le \eta \le 0.812$, but quantum coherences of modes A and B still exist. The quantum coherences of modes A and B both decrease when η increases from zero to 0.5 and increase when η increases from 0.5 to one. The quantum coherences are equal to zero when $\eta = 0.5$ because modes A and B are thermal states that are incoherent states, but they are an EPR entangled state at this point.

Based on the measured covariance matrix $\mathbf{V}_{AB}$, we experimentally quantify the total coherence, local coherence, and correlated coherence according to Eqs. (10), (11), and (12) respectively, which are shown in Fig. 4. The total quantum coherence is equal to local coherence when $\eta = 0$ and $\eta = 1$ because those two Gaussian states of modes A and B are separated at these transmissivities. In this case, the correlated coherence is equal to zero. The correlated coherence is maximal, but the local quantum coherence is equal to zero at $\eta = 0.5$

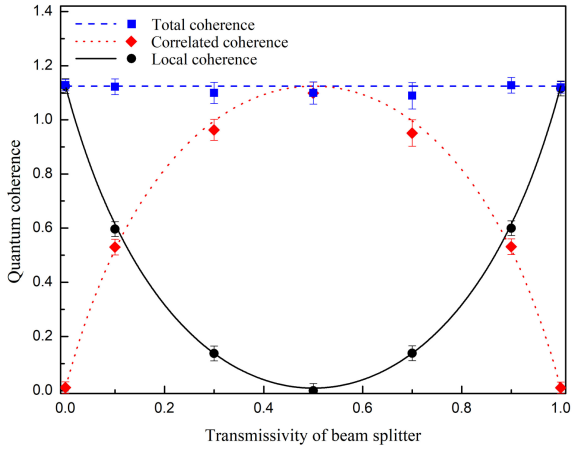

Fig. 4. Dependence of total (dashed blue line), local (solid black curve), and correlated coherence (dotted red curve) of the two-mode Gaussian state on transmissivity of beam splitter. Dots, squares, and diamonds correspond to experimental results.

because modes A and B are an EPR entangled state, but each of these modes is a thermal state that is an incoherent state. The total coherence is composed of correlated coherence totally at $\eta = 0.5$. By comparing quantum coherence at $\eta = 0$ and $\eta = 0.5$, we show that local quantum coherence is converted into correlated quantum coherence when two separable squeezed states are converted into an entangled state.

The total quantum coherence remains unchanged when η increases from zero to one. Local quantum coherence decreases when η increases from zero to 0.5 and increases when η increases from 0.5 to one, while correlated quantum coherence shows the opposite behavior. No matter what the transmissivity is, the total coherence of a two-mode Gaussian state is the sum of local quantum coherence and correlated quantum coherence.

In summary, we experimentally demonstrate the conversion of local and correlated Gaussian quantum coherence along with the conversion from two squeezed states to an entangled state. We show that local coherence exists even when squeezing disappears. We also demonstrate that the total coherence of a two-mode Gaussian state is the sum of local coherence of each mode and correlated coherence between two modes. The presented results clarify the relation among total, local, and correlated coherence of a two-mode Gaussian state and provide references for applications based on quantum coherence.

Funding. National Natural Science Foundation of China (11834010); National Key Research and Development Program of China (2016YFA0301402); Fund for Shanxi "1331 Project" Key Subjects Construction.

Disclosures. The authors declare no conflicts of interest.

Data Availability. Data underlying the results presented in this Letter are not publicly available at this time but may be obtained from the authors upon reasonable request.

REFERENCES

1. T. Baumgratz, M. Cramer, and M. B. Plenio, Phys. Rev. Lett. **113**, 140401 (2014).
2. A. Streltsov, G. Adesso, and M. B. Plenio, Rev. Mod. Phys. **89**, 041003 (2017).
3. E. Chitambar and G. Gour, Rev. Mod. Phys. **91**, 025001 (2019).
4. S. Cheng and M. J. W. Hall, Phys. Rev. A **92**, 042101 (2015).
5. X. Yuan, G. Bai, T. Peng, and X. Ma, Phys. Rev. A **96**, 032313 (2017).
6. Z. Xi, Y. Li, and H. Fan, Sci. Rep. **5**, 10922 (2015).
7. Z.-X. Wang, S. Wang, T. Ma, T.-J. Wang, and C. Wang, Sci. Rep. **6**, 38002 (2016).
8. E. Chitambar and M.-H. Hsieh, Phys. Rev. Lett. **117**, 020402 (2016).
9. K.-D. Wu, Z. Hou, H.-S. Zhong, Y. Yuan, G.-Y. Xiang, C.-F. Li, and G.-C. Guo, Optica **4**, 454 (2017).
10. J. Gao, Z.-Q. Jiao, C.-Q. Hu, L.-F. Qiao, R.-J. Ren, H. Tang, Z.-H. Ma, S.-M. Fei, V. Vedral, and X.-M. Jin, Commun. Phys. **1**, 89 (2018).
11. K.-D. Wu, Z. Hou, Y.-Y. Zhao, G.-Y. Xiang, C.-F. Li, G.-C. Guo, J. Ma, Q.-Y. He, J. Thompson, and M. Gu, Phys. Rev. Lett. **121**, 050401 (2018).
12. H. Xu, F. Xu, T. Theurer, D. Egloff, Z.-W. Liu, N. Yu, M. B. Plenio, and L. Zhang, Phys. Rev. Lett. **125**, 060404 (2020).
13. X. N. Feng and L. F. Wei, Sci. Rep. **7**, 15492 (2017).
14. C. Napoli, T. R. Bromley, M. Cianciaruso, M. Piani, N. Johnston, and G. Adesso, Phys. Rev. Lett. **116**, 150502 (2016).
15. Y.-R. Zhang, L.-H. Shao, Y. Li, and H. Fan, Phys. Rev. A **93**, 012334 (2016).
16. J. Xu, Phys. Rev. A **93**, 032111 (2016).
17. D. Buono, G. Nocerino, G. Petrillo, G. Torre, G. Zonzo, and F. Illuminati, "Quantum coherence of Gaussian states," arXiv: 1609.00913v1 (2016).
18. K. C. Tan, H. Kwon, C.-Y. Park, and H. Jeong, Phys. Rev. A **94**, 022329 (2016).
19. Q. Zheng, J. Xu, Y. Yao, and Y. Li, Phys. Rev. A **94**, 052314 (2016).
20. S.-R. Yang and C.-S. Yu, Ann. Phys. **388**, 305 (2018).
21. H. Cao, C. Radhakrishnan, M. Su, Md. Manirulali, C. Zhang, Y.-F. Huang, T. Byrnes, C.-F. Li, and G.-C. Guo, Phys. Rev. A **102**, 012403 (2020).
22. C. Filgueiras, O. Rojas, and M. Rojas, Ann. Phys. (Berlin) **532**, 2000207 (2020).
23. X.-B. Wang, T. Hiroshima, A. Tomita, and M. Hayashi, Phys. Rep. **448**, 1 (2007).
24. C. Weedbrook, S. Pirandola, R. Garca-Patrón, N. J. Cerf, T. C. Ralph, J. H. Shapiro, and S. Lloyd, Rev. Mod. Phys. **84**, 621 (2012).
25. A. Furusawa, J. L. Sørensen, S. L. Braunstein, C. A. Fuchs, H. J. Kimble, and E. S. Polzik, Science **282**, 706 (1998).
26. M. Huo, J. Qin, J. Cheng, Z. Yan, Z. Qin, X. Su, X. Jia, C. Xie, and K. Peng, Sci. Adv. **4**, eaas9401 (2018).
27. J. Mizuno, K. Wakui, A. Furusawa, and M. Sasaki, Phys. Rev. A **71**, 012304 (2005).
28. X. Li, Q. Pan, J. Jing, J. Zhang, C. Xie, and K. Peng, Phys. Rev. Lett. **88**, 047904 (2002).
29. X. Jia, X. Su, Q. Pan, J. Gao, C. Xie, and K. Peng, Phys. Rev. Lett. **93**, 250503 (2004).
30. N. Takei, H. Yonezawa, T. Aoki, and A. Furusawa, Phys. Rev. Lett. **94**, 220502 (2005).
31. X. Su, C. Tian, X. Deng, Q. Li, C. Xie, and K. Peng, Phys. Rev. Lett. **117**, 240503 (2016).
32. X. Su, W. Wang, Y. Wang, X. Jia, C. Xie, and K. Peng, Europhys. Lett. **87**, 20005 (2009).
33. T. Gehring, V. Händchen, J. Duhme, F. Furrer, T. Franz, C. Pacher, R. F. Werner, and R. Schnabel, Nat. Commun. **6**, 8795 (2015).
34. E. Diamanti, H.-K. Lo, B. Qi, and Z. Yuan, npj Quantum Inf. **2**, 16025 (2016).
35. R. Ukai, N. Iwata, Y. Shimokawa, S. C. Armstrong, A. Politi, J.-I. Yoshikawa, P. van Loock, and A. Furusawa, Phys. Rev. Lett. **106**, 240504 (2011).
36. X. Su, S. Hao, X. Deng, L. Ma, M. Wang, X. Jia, C. Xie, and K. Peng, Nat. Commun. **4**, 2828 (2013).
37. X. Su, M. Wang, Z. Yan, X. Jia, C. Xie, and K. Peng, Sci. China Inf. Sci. **63**, 180503 (2020).
38. F. Albarelli, M. G. Genoni, and M. G. A. Paris, Phys. Rev. A **96**, 012337 (2017).
39. X.-L. Wang, Q.-L. Yue, C.-H. Yu, F. Gao, and S.-J. Qin, Sci. Rep. **7**, 12122 (2017).
40. S. Steinlechner, J. Bauchrowitz, T. Eberle, and R. Schnabel, Phys. Rev. A **87**, 022104 (2013).